Desalination and Water Treatment
www.deswater.com

doi: 10.5004/dwt.2023.29730

300 (2023) 178–191
July

Acacia saligna leaves: a potential new low-cost adsorbent for removal of methylene blue from aqueous solutions

Mohamed Cherif Terkhi*, Ali Belhaine, Fatiha Abdelmalek, Mouffok Redouane Ghezzar, Ahmed Addou

Laboratory of Environmental Science and Valorization, Department of Process Engineering, University Abdelhamid Ibn Badis Mostaganem, BP 188, Mostaganem 27000, Algeria, emails: medcherif.terkhi@univ-mosta.dz (M.C. Terkhi), ali.belhaine@univ-mosta.dz (A. Belhaine), fatiha.abdelmalek@univ-mosta.dz (F. Abdelmalek), redouane.ghezzar@univ-mosta.dz (M.R. Ghezzar), ahmed.addou@univ-mosta.dz (A. Addou)

Received 19 February 2023; Accepted 24 June 2023

ABSTRACT

The objective of this research was to study the capacity of a new biosorbent from *Acacia saligna* leaf powder (ASLP) to remove methylene blue (MB) under varying operating conditions: initial concentration of the dye, the mass of biosorbent, adsorption time, pH, temperature and ionic strength. ASLP surface morphology, structural, and thermal properties were investigated by scanning electron microscopy, Fourier-transform infrared spectroscopy and thermogravimetric analysis, respectively. The study showed the significant role of cellulose, hemicellulose, and lignin, which are rich in functional groups such as –OH, –COOH, and $–NH_2$, in the adsorption mechanism, enabling the effective binding of MB molecules. The Langmuir isotherm model was found to be the most suitable model for describing the experimental data, exhibiting a high coefficient of determination (R^2 = 0.993). At room temperature, the maximum adsorption capacity achieved was 71.43 $mg \cdot g^{-1}$. The pseudo-second-order model (R^2 = 1) provided a better description of the adsorption process of MB by ASLP compared to the pseudo-first-order model (R^2 = 0.86). This observation can be attributed to the formation of a monolayer on the external surface of ASLP. The thermodynamic analysis indicated that the adsorption process was spontaneous, exothermic. The potential for regenerating and reusing the adsorbent was also investigated. The study findings highlight that *A. saligna* leaf powder is a cost-effective biosorbent that is readily accessible and adheres with the principles of green chemistry for the efficient removal of methylene blue from wastewater.

Keywords: Acacia saligna leaves; Methylene blue; Adsorption kinetics; Thermodynamic parameters; Green chemistry

1. Introduction

The various sectors including paper, plastic, leather, textile, food, among others, contribute significantly to pollution and exacerbate water scarcity and water stress. Overall, these industries account for 20% of global water pollution [1]. Among them, the textile industry, along with dyeing, cosmetic, food, pharmaceutical, paper, wood, silk, plastics, and printing industries, is one of the largest consumers of water. However, the textile industry is also a major source of dyes, metals, hazardous substances, and chemicals in wastewater. It is estimated that there are over 100,000 commercially available types of dyes, with an annual production exceeding 800,000 tons [2]. Approximately 30%–40% of these dyes are discharged into industrial wastewater. Discharging untreated or inadequately treated wastewater can have adverse effects on human and animal health. Numerous studies have demonstrated the carcinogenic,

* Corresponding author.

toxic, and harmful nature of dyes, which can lead to various health issues such as allergies, skin irritation, respiratory difficulties, nausea, sweating, vomiting, confusion, high blood pressure, headaches, and mutations. Furthermore, the discharge of these dyes into the environment has a detrimental impact on both ecosystems and the economy [3]. Due to their complex aromatic structures, these dyes are highly stable and pose challenges for natural biodegradation processes. Although biological treatments are commonly used for wastewater decontamination, their effectiveness is limited when it comes to industrial wastewater, particularly those containing dyes [4]. Dyes are known to be recalcitrant to conventional degradation processes. Various physical, chemical, and biological techniques have been developed to eliminate dyes from wastewater, such as traditional methods, advanced oxidation processes, and adsorption. However, these techniques are often specific to certain types of wastewater discharges [5]. Nevertheless, in recent years, bioadsorption has emerged as a highly promising method for dye removal, offering an attractive alternative to conventional adsorbents. This approach is particularly advantageous when the adsorbent is natural, readily available, and cost-effective. Examples of such bioadsorbents include *Moringa oleifera* leaves, oak wood, *Ficus carica* stems, *Melia azedarach* bark, *Juglans regia* shells, algal biomasses, solid waste, agricultural and forestry residues, industrial and food waste, sewage sludge, and fishing waste [6–12]. Biosorption offers several benefits, including its low cost, high efficiency, minimal sludge generation, and the possibility of regenerating and reusing the biosorbent [13].

Methylene blue (MB) is a cationic dye used in the textile industry and medicine, biology, and chemistry. It is not toxic, but it can cause dangerous effects on living organisms (increased heart rate, vomiting, cyanosis, jaundice, eye burns, quadriplegia, tissue necrosis, methemoglobinemia, dyspnea, tachycardia, etc.) [14]. It is considered a standard model for its well-known characteristics in adsorption [15].

This work has the following objectives: (i) to assess and evaluate the effectiveness of a carbon adsorbent derived from *Acacia saligna* leaves, prepared for the first time, for the removal of MB from aqueous solution, (ii) to develop an adsorption-based removal system that adheres to the principles of green chemistry, and (iii) to propose a mechanism for the adsorption of MB by *Acacia saligna* leaf powder (ASLP). This work is devoted to the adsorption of MB using *A. saligna* leaves, for the first time.

The study was carried out according to the characteristic parameters likely to affect the adsorption process (dose of biosorbent, initial concentration of MB, pH of the solution, contact time, ionic strength, and temperature). Kinetic and mass transfer models have been applied for the adsorption of MB on activated carbon.

The adsorption capacity has been determined using Langmuir and Freundlich isotherms. To investigate the type of adsorption, kinetic and thermodynamic experiments were done. The possibility of regenerating the modified biomaterial for reuse was also investigated.

2. Materials and methods

2.1. Study area

A. saligna (Mimosa) is extremely abundant in the city of Mostaganem, located in northwestern Algeria (360 km west of Algiers) (Fig. 1). It can be found in the city and its surroundings throughout the year. During spring and at the end of each summer, the trees are pruned, and the resulting waste is disposed of in large quantities at the city's technical landfill. The idea is to recover this waste and recycle it as a natural biosorbent to remove methylene blue. The leaves of *A. saligna* have been used in powder form, without any physical, chemical, or thermal treatment, in order to minimize costs.

2.2. Description and preparation of bioadsorbent

A. saligna is known as Willow leaf Mimosa or blue leaf Mimosa. It is an invasive plant species, drought-resistant, with low nutritional requirement and tolerance to salinity [16]. The fodder tree is bushy and arborescent forms are used as a windbreaker, dune fixation, agroforestry, wood, etc.

A. saligna leaves were initially washed with water and subsequently rinsed multiple times using distilled water to effectively eliminate any impurities such as soluble matter, fine particles, and dust. Following this cleaning process, the leaves were dried at a temperature of 60°C for 24 h (Fig. 2). The dried leaves were grounded with a domestic mixing grinder and sieved to particle size of 150 μm and stored in a container for further experiments. Various parameters that affect the process of adsorption were examined.

2.3. Reagents and materials

All reagents used were of analytical grade and were obtained from by Merck (Germany). Materials used: scanning electron microscopy (SEM; Hitachi Tabletop Microscope TM-1000, Japan), thermogravimetric analysis (TGA; SDT 650

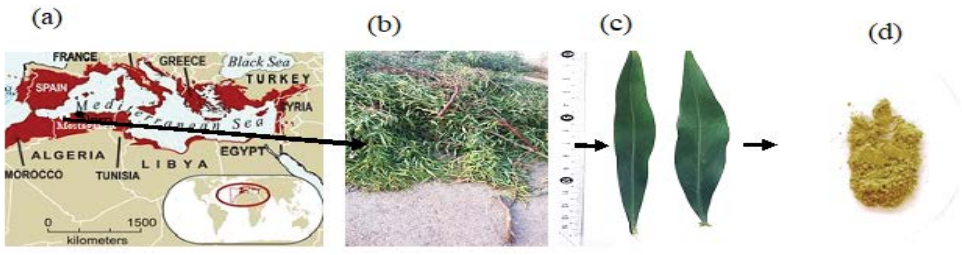

Fig. 1. (a) Collection place of *Acacia saligna* leaves. (b) Tree trunks of *Acacia saligna* cut and abandoned. (c) Leaves of *Acacia saligna* form willow. (d) Leaves of *Acacia saligna* prepared as biosorbent (powder).

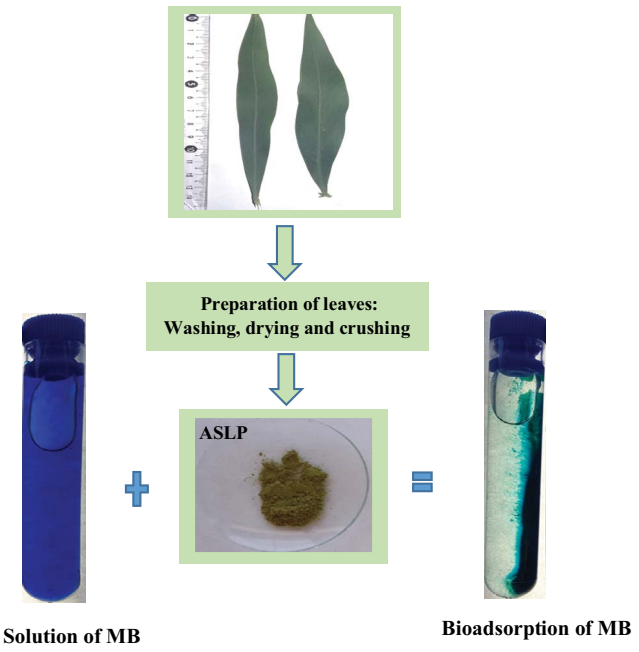

Fig. 2. Adsorption process of methylene blue by *Acacia saligna* leaf powder (ASLP).

- TA Instruments, New Castle, EUA), Fourier-transform infrared spectroscopy (FTIR; Thermo Scientific Nicolet 380, United States), spectrophotometer (OPTIZEN 3220 Double Beam UV/Vis Spectrophotometer, South Korea), pH meter (Mettler Toledo 340, Switzerland), oven (Digital Muffle Furnace Model FHX-05 DAIHAN Scientific, South Korea). The chemical formula of methylene blue is $C_{16}H_{18}ClN_3S$, with a molar mass of 319.87 g and purity greater than 95%. MB solutions were prepared by dissolving an appropriate amount in distilled water.

2.4. Characterization of the adsorbent ASLP

The adsorbent ASLP was characterized by SEM, FTIR and TGA. Additionally, the ash content and the pH value at the point of zero charge (pH_{pzc}) were determined.

2.4.1. pH of the zero-point charge (pH_{pzc})

The pH_{pzc} has been determined by the method of Noh and Schwarz [17]. Doses of 0.3 g of ASLP were introduced into conical flasks containing 50 mL of 0.01 M NaCl. The initial pH of these solutions was modified between 2 and 12 by adding 0.1 M HCl or NaOH. The suspensions are mechanically stirred and maintained at room temperature for 48 h and the final pH is then measured. The pH which corresponds to the point of intersection with the line pHfinal = pHinitial is the pH_{pzc}.

2.4.2. Ash content

1 g of ASLP has been placed in a dry crucible and introduced into a furnace at 500°C for 4 h [18]. The percentage of ash content is given by Eq. (1):

$$\%C = \frac{m_{ash}}{m_{sec}} \times 100 \quad (1)$$

where m_{ash}: mass of ASLP after drying (g) and m_{sec}: mass of ash (g).

2.4.3. FTIR spectroscopy

The samples were prepared in the form of KBr pellets with 1% powder and fixed on a support in the spectrophotometer measurement chamber. FTIR spectra were recorded from 400 to 4,000 cm^{-1} with a resolution of 4 cm^{-1}.

2.4.4. Thermogravimetric analysis

An amount of the ASLP was heated at 10°C/min under a stream of nitrogen (~99.99%) with a flow rate of 50 mL·min^{-1}. The weight loss of the ASLP was monitored as the temperature increased from 0 to 900°C.

2.5. Batch adsorption of methylene blue

A 1,000 mg·L^{-1} stock solution of MB was prepared for the adsorption experiments and diluted to the desired concentration. The batch experiments determined the MB removal kinetics at equilibrium and evaluated the effect of some important parameters such as the pH of the solution and the adsorbent dose. These experiments were conducted at 25°C with a mass of ASLP and stirred at 300 rpm in 50 mL solution for a specific time. The ASLP-MB mixture was centrifuged at 6,000 rpm for 5 min to separate the ASLP from the aqueous solution. After that, the MB concentrations were determined. The absorbance of the filtrate was measured by UV/Vis spectrophotometry at 665 nm. The removal efficiency (%*R*) of dye can be calculated from Eq. (2):

$$\%\text{Removal efficiency} = \frac{C_0 - C_e}{C_0} \times 100 \quad (2)$$

where C_0 and C_e (mg·L^{-1}) are the initial and final concentrations of MB in the supernatant. The adsorption capacity (q) is given by Eq. (3):

$$q = \frac{(C_0 - C_e)V}{m} \quad (3)$$

where q (mg·g^{-1}) is the quantity of the dye adsorbed, V (L) is the volume of the dye solution and m (g) is the mass of ASLP.

2.5.1. Effect of bioadsorbent dosage

The effect of the optimal amount of ASLP was evaluated by conducting the following experiments: 50 mL of MB solution (100 mg·L^{-1}) was added to different ASLP concentrations ranging from 2 to 16 g·L^{-1}.

2.5.2. Effect of pH

To evaluate this effect, pH was adjusted with a within the pH range of 2–9. An optimum mass of 0.3 g of ASLP was added to 50 mL of MB (100 mg·L^{-1}) and stirred (300 rpm) for 20 min.

2.5.3. Kinetic and isotherms studies

The optimal contact time was determined by introducing 0.3 g ASLP in 50 mL at the initial 100 mg·L^{-1} concentration and pH = 6.7. Biosorption of the dye was achieved up to 40 min at a mixing speed of 300 rpm.

Adsorption isotherms were determined using thirteen different initial concentrations of MB, ranging from 60 to 500 mg·L^{-1}. The ASLP-MB mixture was stirred during 20 min. The dose of adsorbent and the pH of the aqueous solution were fixed respectively at 6 g·L^{-1} and natural pH = 6.7.

2.5.4. Effect of temperature

The influence of temperature was studied at different temperatures: 30°C, 40°C, and 50°C. This study was conducted using a solution containing 6 g·L^{-1} of ASLP and 100 mg·L^{-1} of MB.

2.5.5. Effect of ionic strength by NaCl

The influence of salt concentration on the adsorption ability of ASLP was studied by addition of NaCl to the MB solution in range from 0.0125 to 0.2 M.

2.5.6. Desorption studies

Adsorption/desorption studies were conducted to analyse the possibility of reusing the adsorbent for further adsorption and to make the process more economical. Regeneration studies were carried out by gently washing the adsorbent with distilled water to remove unadsorbed MB. 50 mL of 0.1 M HCl solution was used and the solution was stirred for 24 h. Then, the solution was analyzed using a UV-Vis spectrophotometer at 665 nm. After desorption process, ASLP was washed several times with distilled water, dried at 80°C and was used for the next adsorption–desorption cycle experiment at 25°C.

MB adsorption–desorption was performed for four cycles. The MB desorption rate was obtained using the following equation:

$$\%\text{Dye desorption} = \frac{q_{\text{desorption}}}{q_{\text{adsorption}}} \times 100 \quad (4)$$

3. Results and discussion

3.1. Characterization of ASLP

3.1.1. pH_{pzc}

The pH of zero-point charge (pH_{pzc}) is an essential and significant parameter in understanding adsorption phenomena, particularly in estimating the acid-base nature of a solution. Adsorption mechanisms involve the participation of electrostatic forces. The pH_{pzc} represents the pH value at which the surface charge of the adsorbent becomes neutral [19]. The adsorption of cation is favored at pH > pH_{pzc} and the adsorption of anion is favored at pH < pH_{pzc}. The pH which corresponds to the point of intersection with the line pH_{final} = $pH_{initial}$ is the pH_{pzc}, in our study, it found to be equal to 6.5 (Fig. 3). At a pH above the pH_{pzc}, the surface of the adsorbent becomes more negatively charged by losing protons. Therefore, the adsorption of the MB reached its maximum value in the higher pH because of strong electrostatic attractions between the negatively charged surface of the ASLP and the cationic MB. At a pH below the pH_{pzc}, the surface of the adsorbent is positive (6.5), the adsorption capacity of MB decreases due to repulsion between the positively charged surface of ASLP and the positively charged MB molecules. However, the adsorption of MB onto ASLP can still occur through an electrostatic attraction between negatively charged functional groups present on the surface of the adsorbent and the positively charged dye molecules. Since the pH value of the ASLP-MB mixture was 6.7, which is close to the pH_{pzc} of 6.5, no pH adjustment was required for the next experiments.

3.1.2. Ash content

The ash content is a useful parameter for assessing the activity potential of an adsorbent as it determines the mineral matter present in the material. The low ash content value of 9% observed in ASLP suggests a limited presence of metallic elements that could lead to the formation of metal oxides during the calcination process. It is desirable for an adsorbent to have a low ash content, as this indicates higher purity and effectiveness [20]. However, it's important to note that the ash content can have certain effects. First, it can increase the hydrophilicity of the adsorbent, which acquires catalytic properties. As a result, the regeneration process of the used adsorbents will be promoted, and a restructuring effect will take place [21].

3.1.3. FTIR analysis

Infrared spectroscopy provides information on the chemical structure. It describes changes in functional groups (hydroxyl, carbonyl, amines, etc.) after adsorption reaction

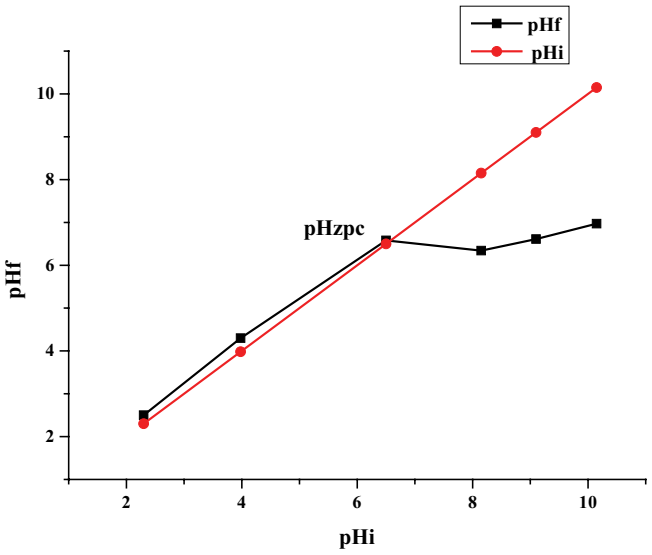

Fig. 3. Graphical representation of the pH_{pzc} of ASLP.

[22]. Fig. 4 illustrates the FTIR spectra of ASLP before and after adsorption of MB. The peaks observed in the spectra correspond to various functional groups and bonds, indicating the complex nature of the biosorbent. These findings provide insights into the interactions occurring during the adsorption process.

The spectrum of untreated ASLP is similar to the one of the raw leaves [23,24]. Free or hydrogen bonded O–H groups and $–NH_2$ groups are characterized by absorption peaks around 3,000–3,500 cm^{-1}. A broad and strong band stretching vibration of $–NH_2$ groups and free and/or hydrogen bonded O–H groups (alcohols primary and secondary, carboxylic acids and phenols) was observed at 3,338 cm^{-1} [24]. The peaks at 2,916 and 2,848 cm^{-1} indicate the C–H stretching symmetric and asymmetric mode of aliphatic compounds. The intense and fine peak at 1,620 cm^{-1} is attributed to the C=C stretching of aromatic bonds and carboxylate groups ($–COO^-$) [25]. The low intensity peak at 1,529 cm^{-1} corresponds to the N–H deformation of secondary amines. The medium intensity peak at 1,444 cm^{-1} is assigned to the C–O bond stretching of the carboxyl groups. The low intensity peak observed at 1,369 cm^{-1} shows the presence of phenolic group. The peak at 829 cm^{-1} indicates the presence of C–H groups [23]. The frequencies at 1,368 and 1,236 cm^{-1} can be assigned to the symmetric stretching of –COO, the deformation of –CO and the stretching of –OH in carboxylic acids. The band at 1,037 cm^{-1} is due to C–O deformation vibration of carboxylic acids, alcohols and ethers groups. The peak at 673 is attributed to the out-of-plane stretching of C–H in aromatic derivatives. The frequencies 1,145 and 1,107 cm^{-1} are due to C–O or C–N groups and possibly sugar varieties [26].

Fig. 4a illustrates the presence and availability of several groups, including hydroxyl, amino, and carbonyl, on the surface of ASLP. These functional groups play a significant role in influencing the adsorption capacity of ASLP. The availability and accessibility of these groups determine the binding sites and interactions with the adsorbate (MB in this case). The presence of hydroxyl, amino, and carbonyl groups provides potential sites for adsorption and facilitates the process, thereby affecting the overall adsorption capacity of ASLP.

The modifications observed in the spectrum of ASLP (Fig. 4b) after the adsorption of MB indicate changes in the frequencies of absorption bands associated with various functional groups. These modifications can be attributed to the involvement of these functional groups in the adsorption process, either through the formation of chemical bonds or through Van der Waals forces [27]. (i) Chemical bond formation occurs when the adsorbate (MB) interacts with the adsorbent surface (ASLP) and forms covalent bonds with the functional groups present on ASLP. This interaction leads to changes in the energy levels of the involved bonds, resulting in shifts in the absorption frequencies observed in the spectrum. The specific nature of these chemical interactions depends on the chemical properties of both the adsorbate and adsorbent. (ii) Van der Waals forces are weak intermolecular forces that arise due to fluctuations in electron distribution within molecules. These forces can contribute to the adsorption process by inducing attractive interactions between the adsorbate and adsorbent. Such interactions may cause changes in the vibrational modes of the functional groups, leading to shifts in the absorption frequencies in the spectrum.

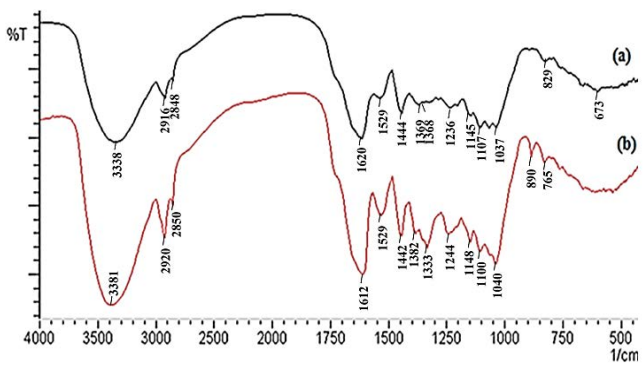

Fig. 4. Fourier-transform infrared spectrum before (a) and after (b) interaction ASLP-MB.

The shift from 3,338 to 3,381 cm^{-1} in the absorption band can be attributed to the hydrogen bonding effect between the nitrogen (N) atoms of MB and the hydroxyl and amino groups of ASLP. Hydrogen bonding occurs when a hydrogen atom forms a weak bond with a highly electronegative atom (such as oxygen or nitrogen) that has lone pair electrons. In this case, the N atoms of MB likely form hydrogen bonds with the hydroxyl and amino groups of ASLP.

The hydrogen bonding interaction can lead to changes in the vibrational modes of the involved functional groups, resulting in a shift in the absorption frequency. The shift to a higher frequency (3,381 cm^{-1}) suggests a strengthening of the hydrogen bonding interaction compared to the original state (3,338 cm^{-1}). This shift indicates a modification in the energy levels and forces acting within the hydrogen bond. The proposition suggests the possibility of a π–π interaction between the aromatic rings of MB and those of lignin present in ASLP. Aromatic rings are composed of delocalized π electrons above and below the plane of the ring. When two or more aromatic systems come close to each other, their π electrons can interact through a phenomenon known as a π–π interaction. In the case of MB and ASLP, the aromatic rings of MB and the lignin components of ASLP may undergo π–π interactions. This interaction can result in attractive forces between the aromatic systems, influencing the adsorption process and leading to changes in the spectroscopic data. The π–π interaction is a non-covalent interaction that can occur between aromatic systems even in the absence of direct chemical bonding.

The shift of the –COO peak from 1,620 to 1,612 cm^{-1} shows the fixation of MB to ASLP by electrostatic attraction. The identical observation was reported by Han et al. [28] and Terkhi et al. [29]. Finally, the shifts of the bands (–OH, –NH and –COOH) show the participation of these functional groups, in the adsorption of dyes by raw leaves. Interactions and ions exchanges with the $–OH$, $–COO^-$, amine and amide functions are responsible for the high adsorption of MB by ASLP.

3.1.4. SEM analysis

The micrograph (Fig. 5) shows that the ASLP composes of micrometric agglomerated particles. Fig. 5a (x2.0K)

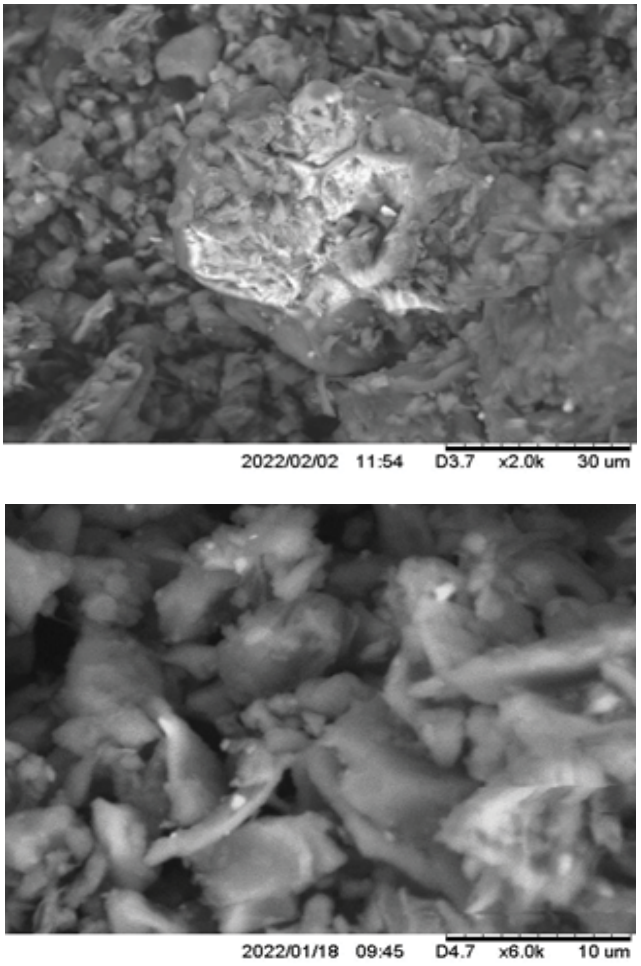

Fig. 5. Scanning electron microscopy image of ASLP with several magnifications (a) X2.0K and (b) X6.0K.

shows a heterogeneous and rough surface. The enlarged image (x6.0K) showed that the particles were arranged in different layers in the form of random flakes showing some cavities [30].

3.1.5. TGA analysis

Thermal analysis is a technique employed to assess the changes in chemical, physical, and structural properties of a material in response to temperature variations. Temperature, being a fundamental state variable, plays a pivotal role in influencing various aspects such as chemical reactions, physical properties, and structural transformations. To investigate these changes, thermogravimetric analysis (TGA) was carried out.

The mass loss is caused by the release of vapor/gas, vaporisation of liquids, sublimation, and chemical decomposition [31]. Fig. 6 presents the main stages of the TGA analysis. It also shows the mass loss that has occurred as a function of time and temperature.

- The phase I is composed of two main subsections: The first subsection is characterized by a small weight loss (6.60%) corresponding to the evaporation of moisture where the temperature varied from 30°C to125°C. The second subsection corresponds to the temperature zone between 110°C and 200°C corresponding to the evaporation of chemisorbed water (7.2% weight loss) and volatile substances.
- The phase II at temperature range between 200°C and 500°C (3.43% weight loss), the degradation of hemicellulose and cellulose [32].
- Phase III is the tailing section of the TGA curve characterized by the slow decomposition of lignin starting at 500°C up to 900°C (16% weight loss) [33].

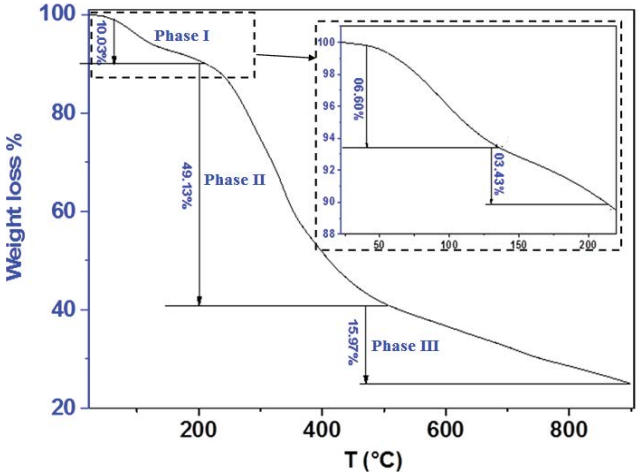

Fig. 6. Thermogravimetric analysis for ASLP.

3.2. Effect of several parameters on the adsorption of MB

3.2.1. Effect of pH

The pH has an impact on the biosorbent surface, indicating its surface charge and the degree of ionization of the dye [34]. It also influences the structural stability and color intensity of MB. Fig. 7 illustrates the correlation between pH and the removal of the dye within the pH range of 2–9. The experiments were carried out using solutions containing 6 g·L^{-1} of ASLP and 100 mg·L^{-1} of MB at different pH values.

All other parameters were maintained constant (contact time: 20 min; temperature: 25°C and stirring speed: 300 rpm). The maximum amount bioadsorbed is obtained for pH 6.7.

Adsorption increases with increasing pH due to deprotonation, which reduces charge density and enhances biosorption. At higher pH values, the surface layer of ASLP tends to become neutralized due to a significant decrease in protons, thereby reducing the effect of adsorption through lower electrostatic attraction forces [28,35].

3.2.2. Effect of adsorbent dose

Batch sorption experiments were performed to study the effect of ASLP on MB adsorption. Different amounts of ASLP ranging from 2 to 19 g·L^{-1} were added to 50 mL of 100 mg·L^{-1} MB (the other parameters were maintained

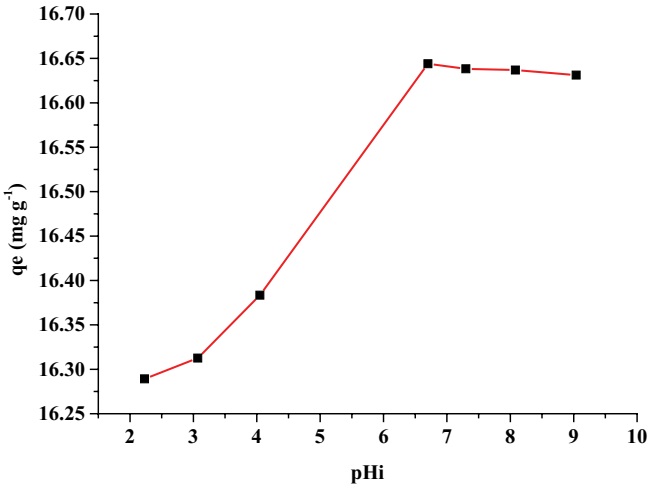

Fig. 7. Effect of pH on the adsorption of methylene blue (*C*: 100 mg·L^{-1}; dose: 6 g·L^{-1}; contact time: 20 min; temperature: 25°C and stirring speed: 300 rpm).

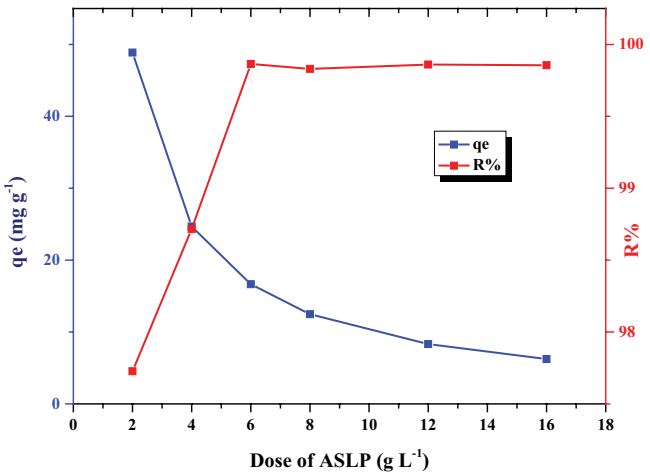

Fig. 8. Effect of adsorbent dose (*C*: 100 mg·L^{-1}; contact time: 20 min; temperature: 25°C and stirring speed: 300 rpm).

constant). The adsorption sites can be optimized by increasing the adsorbent dose and assessing number of sorption sites accessible for adsorbate–adsorbent interaction.

The results (Fig. 8) show an increase in the rate of adsorption of MB by increasing the dose of ASLP from 97.7% to 99.8% when the amount of ASLP increases from 2 to 6 g.

The adsorption capacity of MB exhibits a rapid decrease from 48.86 to 8.32 mg·g^{-1} as the biosorbent dose increases, followed by a slight decrease to 6.24 mg·g^{-1}, and stabilizes at a constant value. This can be attributed to the disparity in concentration between the suspended biosorbent and the biosorbent's surface. When the ratio between initial adsorbent dosage and adsorbate concentration is low, the available active sites are more efficiently utilized. Another potential factor could be the overlap or aggregation of the available surface area of the adsorbent for MB adsorption, resulting in an increase in the length of the diffusion path [36]. The elimination rate of MB reached 99.8% (Fig. 8) when

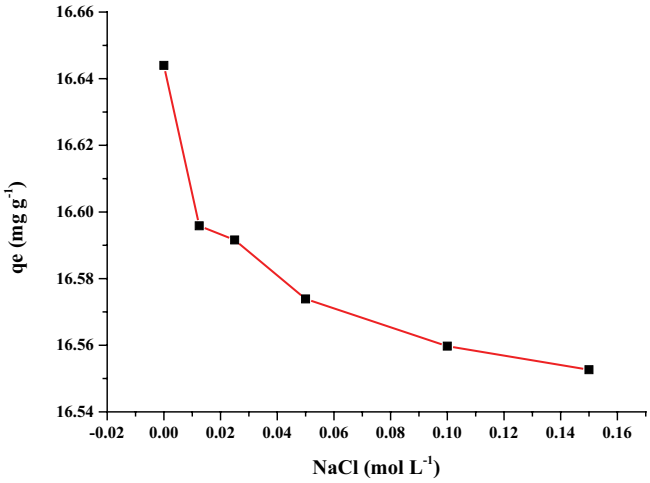

Fig. 9. Effect of ionic strength (*C*: 100 mg·L^{-1}; dose: 6 g·L^{-1}; contact time: 20 min; temperature: 25°C and stirring speed: 300 rpm).

using the optimal dose of 6 g·L^{-1} of ASLP. These results agree with the work of Ouldmoumna et al. [35] and Zou et al. [36], who respectively studied the removal of MB on *Eucalyptus globulus*, *Cynara cardunculus* and *Prunus cerasifera* leaves by sawdust. Increasing the dose of adsorbent induced an increase in dye removal.

3.2.3. Effect of ionic strength

The presence of ionic species, such as chlorides, nitrates, carbonates, sulfates, etc., commonly found in textile industry wastewater, can have various effects on the charges of the biosorbent. These effects include screening, retention, inhibition, or scavenging. This is due to the fact that wastewater contains different types and concentrations of salts, which contribute to a high ionic strength, thereby influencing the adsorption process [37]. To investigate the impact of salts, specifically NaCl, on the adsorption process, different concentrations ranging from 0.01 to 0.2 mol·L^{-1} were studied. Fig. 9 illustrates the relationship between NaCl concentration in the MB solution and the adsorption capacity. It can be observed that the adsorption capacity gradually decreases as the NaCl concentration increases, reaching a minimum limit of 16.55 mg·g^{-1}.

The removal of the dye has been effective at high salt concentrations (>0.73 g), which is an advantage for adsorption in a highly saline solution. This can be attributed to the low competition between the positively charged MB molecules and Na^+ ions for the accessible adsorption sites [38].

3.2.4. Contact time and kinetics

Fig. 10 shows the removal of MB (100 mg·L^{-1}) by ASLP (dose: 6 g·L^{-1}) as a function of contact time. The results indicate that the adsorption process can be divided into two phases. The first phase, occurring within the initial 10 min, demonstrates rapid kinetics due to the abundance of active sites on the ASLP surface. During this phase, the adsorption of MB onto the biosorbent is highly efficient. The second phase is characterized by a gradual decrease in the

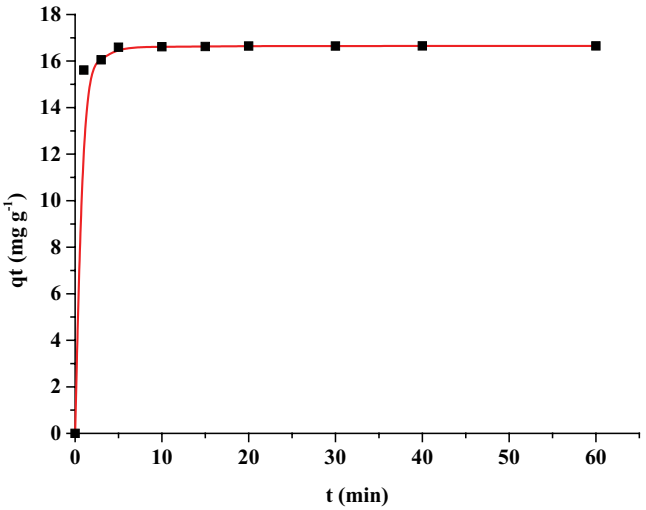

Fig. 10. Effect time on adsorption of methylene blue by ASLP (*C*: 100 mg·L^{-1}; dose: 6 g·L^{-1}; temperature: 25°C and stirring speed: 300 rpm).

rate of interactions, eventually reaching adsorption equilibrium after approximately 20 min of contact. Beyond this point, increasing the contact time has no significant effect on the biosorption process. This slower step is considered quantitatively negligible and can be attributed to the progressive occupation of the available sites on the surface of ASLP, leading to saturation and a decrease in the overall adsorption process [23].

In order to understand the adsorption process, the kinetics of the adsorption rate of MB on the surface of ASLP was studied at various contact times (0–40 min). The obtained results were applied to the three most commonly used models: the pseudo-first-order model [39], the pseudo-second-order model [40], and the intraparticle diffusion model [41].

3.2.4.1. Pseudo-first-order model

The pseudo-first-order model proposed by Lagergren assumes that the adsorption process occurs at a rate proportional to the concentration of the dye. It is represented by the following differential Eq. (5):

$$\frac{dq_t}{dt} = \left(q_e - q_t\right) \tag{5}$$

and an integral form [Eq. (6)]:

$$\ln\left(q_e - q_t\right) = \ln q_e - K_1 t \tag{6}$$

where q_e and q_t (mg·g^{-1}) are the amount adsorbed of dye at equilibrium and at time t (min), respectively. K_1 is the pseudo-first-order adsorption rate constant (min^{-1}). This model is particularly adapted to low concentrations.

3.2.4.2. Pseudo-second-order model

Pseudo-second-order kinetic supposes that rate is an exchange reaction resulting from the adsorption process. It is formulated by the following differential Eq. (7):

$$\frac{dq_t}{dt} = K_2\left(q_e - q_t\right)^2 \tag{7}$$

and in linear form [Eq. (8)].

$$\frac{t}{q_t} = \frac{1}{K_2 q_e^2} + \frac{1}{q_e} t \tag{8}$$

where q_t (mg·g^{-1}) is the amount of MB adsorbed at time t (min), q_e (mg·g^{-1}) is the equilibrium adsorption capacity, K_2 (g·mg^{-1}·min^{-1}) the pseudo-second-order rate constant of adsorption.

3.2.4.3. Intraparticle diffusion model

Weber and Morris used an intraparticle diffusion model to describe the adsorption process by Eq. (9):

The intraparticle diffusion model proposed by Weber and Morris has been applied to describe the adsorption process. The model is given by Eq. (9):

$$q_t = K_i t^{1/2} + C \tag{9}$$

where q_t (mg·g^{-1}) is the amount adsorbed of dye at equilibrium, K_i (mg·g^{-1}·min$^{-1/2}$) is the intraparticle diffusion rate constant and C (mg·g^{-1}) is a constant regarding the thickness of the boundary layer, which is in direct ratio to the effect of the boundary layer.

The experimental data (Fig. 11) were adequately fitted with these models (Table 1). The calculated q_{cal} values obtained from the pseudo-second-order model is close to the experimental q_{exp} values, indicating that this model is particularly suitable ($R^2 = 1$).

This finding demonstrates the influence of ASLP and MB concentrations on the adsorption rate. According to the pseudo-second-order model, there is an initial rapid reaction that quickly reaches equilibrium, followed by a slower reaction that can continue over time.

The significantly higher value of K_2 (1.2) compared to K_1 (0.21) confirms the MB adsorption process by ASLP. The results of the intraparticle diffusion are presented in Fig. 11c. It can be observed that the adsorption process occurs in two steps: a rapid adsorption stage followed by a slower adsorption rate, which can be attributed to reaching the final equilibrium stage. Thus, the maximum level of adsorption is achieved at the initial phase of the adsorption process. Similar findings have been observed in the adsorption of MB using various natural biosorbents derived from different raw leaves [42].

3.2.5. Adsorption isotherms

An adsorption isotherm describes the equilibrium of adsorption of a substance on a surface at a constant temperature. It represents the relationship between the adsorbate in the surrounding phase and adsorbate adsorbed on the surface of the adsorbent. Adsorption isotherm is essential to describe how solutes interact with adsorbents and to optimize the use of adsorbents [43].

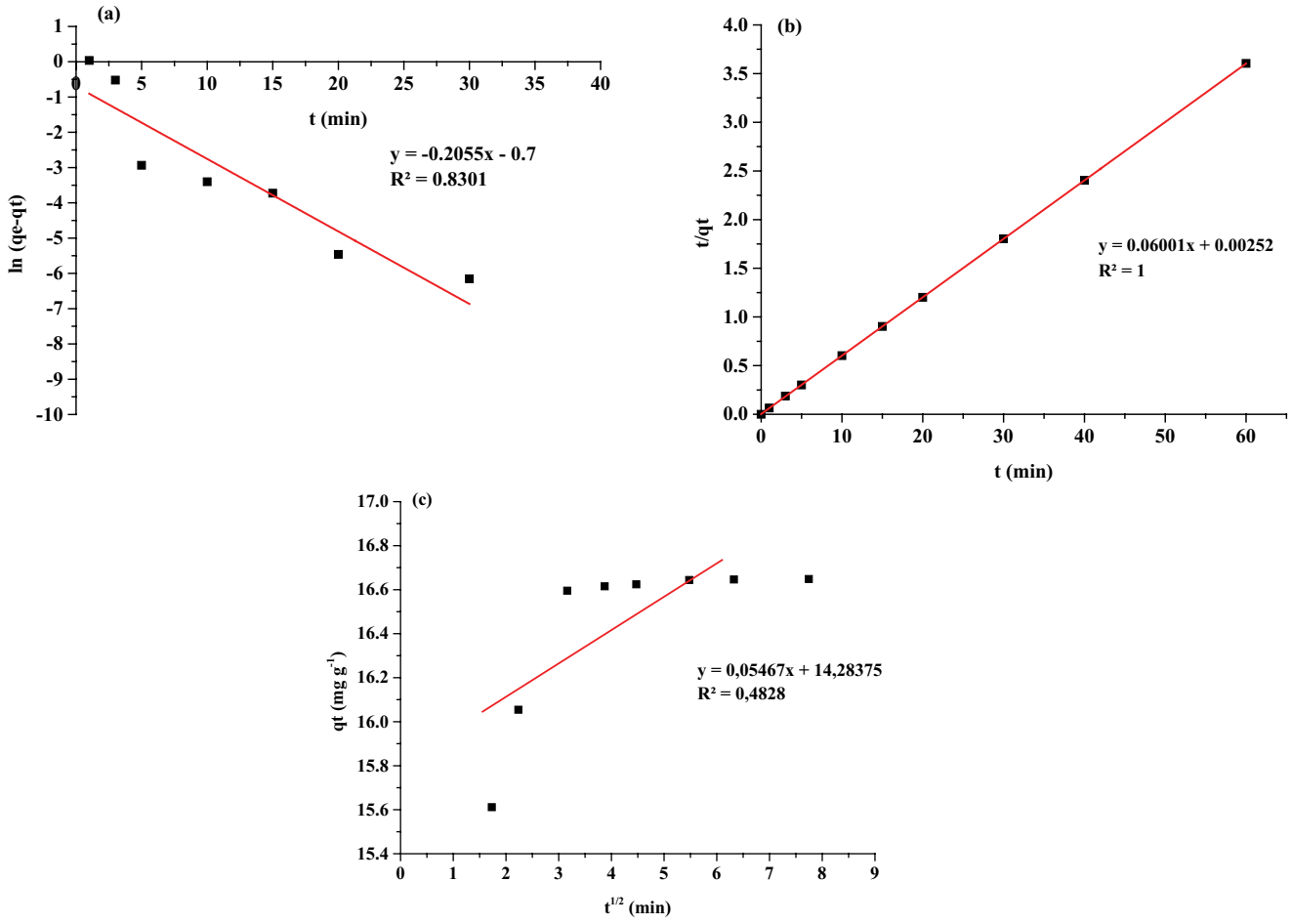

Fig. 11. Kinetics curves for the adsorption process: (a) pseudo-first-order, (b) pseudo-second-order and (c) intraparticle diffusion (*C*: 100 mg·L^{-1}; dose: 6 g·L^{-1}; temperature: 25°C and stirring speed: 300 rpm).

Table 1
Parameters of the kinetics of methylene blue adsorption by ASLP

q_{exp} (mg·g^{-1})	Pseudo-second-order			Pseudo-first-order			Intraparticle diffusion		
16.65	q_{cal} (mg·g^{-1})	K_2 (mg·g^{-1}·min^{-1})	R^2	q_{cal} (mg·g^{-1})	K_1 (min^{-1})	R^2	C (mg·g^{-1})	K_i (mg·g^{-1}·min$^{-1/2}$)	R^2
	16.67	1.20	1	0.50	0.21	0.86	15.99	0.11	0.48

In the present study, the Langmuir and Freundlich models were applied to describe the adsorption equilibrium.

The experiments were carried out by adding 0.3 g of adsorbent in 50 mL of MB solution (60–500 mg·L^{-1}) at a temperature 25°C for a predetermined time (20 min).

The Langmuir model assumes a homogeneous biosorbent surface with a restricted number of adsorption sites. It suggests that only a monolayer is formed during the adsorption process, and the adsorbate molecules occupy these specific surface sites without interacting with each other and with equal affinity. The Langmuir model is represented by Eq. (10) [44]:

$$q_e = \frac{q_{max} K_L C_e}{1 + K_L C_e} \tag{10}$$

where q_e represents the amount of MB adsorbed per unit mass of ASLP (mg·g^{-1}) at equilibrium, C_e the MB concentration (mg·L^{-1}) at equilibrium.

q_{max} (mg·g^{-1}) represents the maximum amount of adsorption and K_L (L·mg^{-1}) the interaction constant (ASLP-MB). Eq. (10) can be rearranged (11):

$$\frac{C_e}{q_e} = \frac{C_e}{q_{max}} + \frac{1}{K_L q_{max}} \tag{11}$$

where q_{max} and K_L are determined from plotted between C_e/q_e vs. C_e.

The form of the Langmuir isotherm can also be described using the separation factor (R_L), which is calculated using Eq. (12) [8]:

$$R_L = \frac{1}{1 + K_L C_0} \quad (12)$$

The Freundlich model is the oldest relation describing the adsorption equation. It is often expressed by Eq. (13):

$$q_e = K_F C_e^{1/n} \quad (13)$$

where q_e is the amount of MB adsorbed per unit mass of ASLP (mg·g^{-1}) at equilibrium, C_e is equilibrium concentration dye in solution (mg·L^{-1}). K_F is a Freundlich constant representing the adsorption capacity, n is the intensity of the adsorption constant and $1/n$ is associated with the surface heterogeneity [38]. Eq. (13) can be linearized according to Eq. (14):

$$\ln q_e = \ln K_F + \frac{1}{n} \ln C_e \quad (14)$$

where K_F and $1/n$ are determined from plotted logq_e vs. logC_e.

Fig. 12 was used to determine the parameters of the Langmuir and Freundlich isotherm models, namely q_{max} and K_L for the Langmuir model, and K_F and $1/n$ for the Freundlich model. These parameter values are presented in Table 2. The Langmuir model exhibited a higher correlation coefficient (R^2 = 0.993) compared to the Freundlich model (R^2 = 0.924). The calculated maximum adsorption capacity (q_{max}) of 71.43 mg·g^{-1} closely matched the experimental value of 69.79 mg·g^{-1} (Table 2). This suggests that the surface of ASLP is homogeneous and that a monolayer of MB covers the surface of adsorbent after adsorption, as indicated by the close agreement between the predicted q_{max} value from the Langmuir model and the experimental value [45]. Han et al. [46] conducted a study on the adsorption of MB dye using the leaves of the phoenix tree. They concluded that the adsorption process followed the Langmuir model, suggesting the formation of a monolayer on the leaf surface. The maximum adsorption capacity they observed was 80.9 mg·g^{-1}. Bhattacharyya and Sharma [47] conducted a similar study using neem leaves. Their results showed a maximum single-layer adsorption capacity of 19.61 mg·g^{-1} for the neem leaves.

The parameter "n" can be used to determine the nature of adsorption. If the value of "n" is equal to 1, it indicates linear adsorption. If "n" is greater than 1, it suggests a physical adsorption process, and if "n" is less than 1, it indicates a chemical adsorption process. In this case, the value of "n" found in Table 2 is 3.46, which is greater than 1. This suggests that the adsorption of MB dye on the ASLP (presumably the material being studied) surface is a physical process [48]. Furthermore, the R_L (separation factor) has been calculated from the Langmuir plot. The R_L value, which falls between 0 and 1, is shown in Fig. 13. An R_L value within this range indicates a favorable adsorption process of MB dye on ASLP [8].

3.2.6. Thermodynamics parameters

Thermodynamic parameters are indicators of the possible nature of adsorption. The Gibbs free energy change ($\Delta G°$), enthalpy change ($\Delta H°$) and entropy change ($\Delta S°$) were calculated according to Eqs. (15) and (16) [36]:

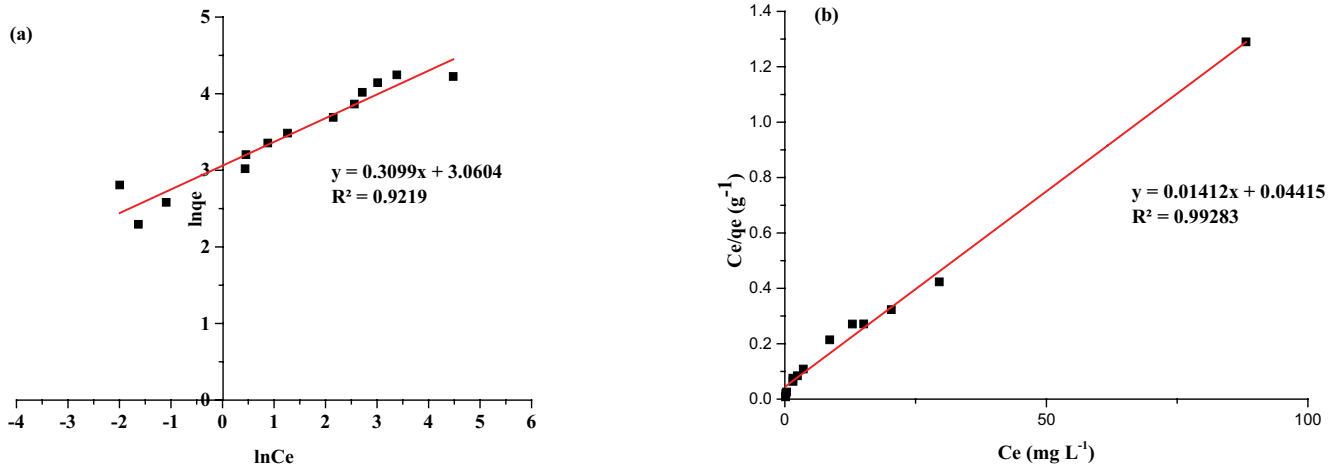

Fig. 12. Isotherms modeling using: (a) Freundlich and (b) Langmuir (C: 100 mg·L^{-1}; dose: 6 g·L^{-1}; contact time: 20 min; temperature: 20°C and stirring speed: 300 rpm).

Table 2
Isotherms parameters of adsorption of methylene blue by ASLP

Langmuir isotherm parameters			q_{exp} (mg·g^{-1})	Freundlich isotherm parameters		
q_m (mg·g^{-1})	K_L (L·mg^{-1})	R^2	69.79	n	K_F (mg·g^{-1})	R^2
71.43	0.297	0.993		3.46	22.49	0.924

$$\Delta G^\circ = \Delta H^\circ - T\Delta S^\circ \quad (15)$$

$$\ln K_d = \frac{\Delta S^\circ}{R} - \frac{\Delta H^\circ}{RT} \quad (16)$$

where K_d is distribution coefficient, R is the universal gas constant (8.314 × 10^{-3} kJ·mol^{-1}·K^{-1}), T is absolute temperature of the solution. Fig. 14 gives lnK_d as a function of 1/T to obtain ΔH° and ΔS° from the slope and its intersection, respectively. The values of thermodynamics parameters are summarized in Table 3. The negative value ΔG° indicates that the adsorption of MB dye on the ASLP surface is possible and spontaneous, regardless of temperature. This suggests that there is a strong affinity between methylene blue and the biosorbents. The negative value of ΔH° indicates that the overall adsorption process is exothermic. This means that the lower temperatures facilitate the adsorption process. The negative value of ΔS° suggests a decrease in efficiency at the solid-solution interface during the adsorption process. This means that the system becomes less disordered or less random during adsorption. These thermodynamic parameters can help in understanding the energetics and efficiency of the adsorption of MB dye on the ASLP surface [49].

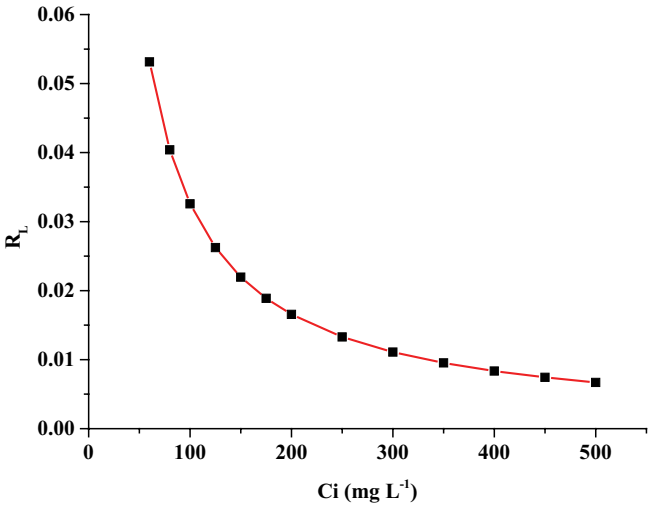

Fig. 13. Value of R_L for biosorption of methylene blue on ASLP.

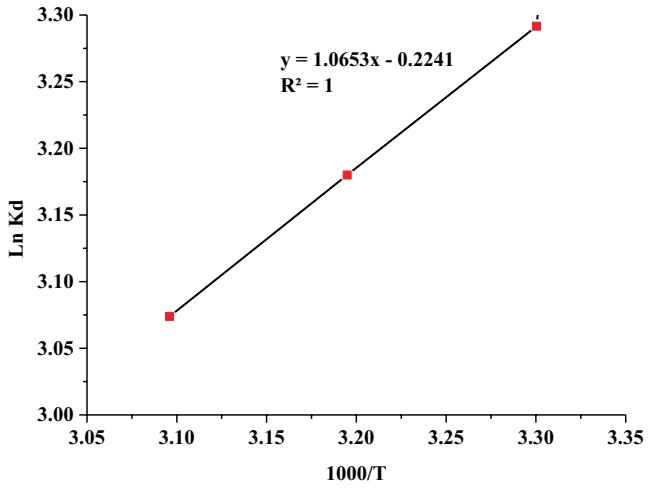

Fig. 14. Effect of temperature on the adsorption of methylene blue (C: 100 mg·L^{-1}; dose: 6 g·L^{-1}; contact time: 20 min and stirring speed: 300 rpm).

3.3. Comparison of ASLP with other raw lignocellulosic adsorbents for MB

Currently, lignocellulosic biomass is used for the biosorption of MB dye due to its hydroxyl and carbonyl functional groups, low cost, biodegradability, and surface morphology [31,50]. In Table 4, the maximum adsorption capacities of several crude lignocellulosic biosorbents are listed. It is noteworthy that the adsorption capacity of ASLP (71.43 mg·g^{-1}) is comparable to values reported in the literature for other materials, such as phoenix tree leaves (80.9 mg·g^{-1}) [26] and *Calotropis* seed pods (88.36 mg·g^{-1}) [51]. The adsorption capacity of *A. saligna* is almost twice as high as that of forest waste (*Salix alba* L.) (35.46 mg·g^{-1}) [50] and *Ipomoea carnea* wood (39.37 mg·g^{-1}) [30]. Moreover, it is approximately four times greater than that of neem leaves (19.61 mg·g^{-1}) [47] and spent *Salvia officinalis* (16.53 mg·g^{-1}) [49]. Notably, the adsorption capacity of ASLP is ten times higher than that observed for *Ficus palmata* leaves (6.89 mg·g^{-1}) [52].

3.4. Proposed mechanisms for the adsorption of MB dye over ASLP

The FTIR study demonstrated that ASLP contained active sites, particularly oxygenated groups on its surface

Table 3
Thermodynamic parameters for methylene blue adsorption on ASLP

Adsorbent	ΔH° (kJ·mol^{-1})	ΔS° (J·mol^{-1}·K^{-1})	ΔG° (kJ·mol^{-1})		
			303 K	313 K	323 K
ASLP	–8.85	–1.86	–8.29	–8.27	–8.25

Table 4
Maximum adsorption capacities similar of various raw lignocellulose adsorbents for methylene blue

Bioadsorbent	q_{max} (mg·g^{-1})	References
Calotropis seed pods	88.36	[51]
Phoenix leaves	80.90	[26]
A. saligna leaves	71.43	This study
Sugarcane bagasse	49.26	[53]
Forest waste (*Salix babylonica*)	42.74	[50]
Palm-trees waste	39.50	[54]
Ipomoea carnea wood	39.37	[30]
Forest waste (*Salix alba* L.)	35.46	[50]
Neem leaves	19.61	[47]
Spent *Salvia officinalis*	16.53	[49]
Ficus palmata leaves	6.89	[52]

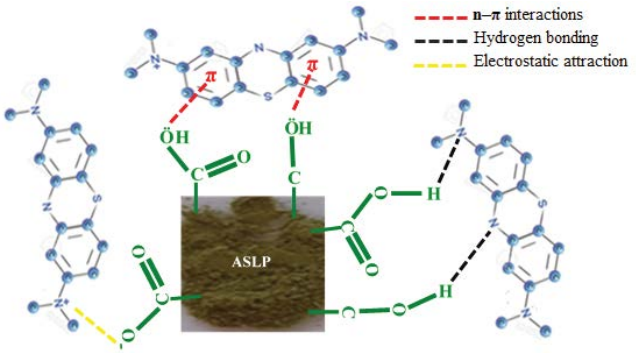

Fig. 15. Proposed adsorption mechanisms of methylene blue by ASLP.

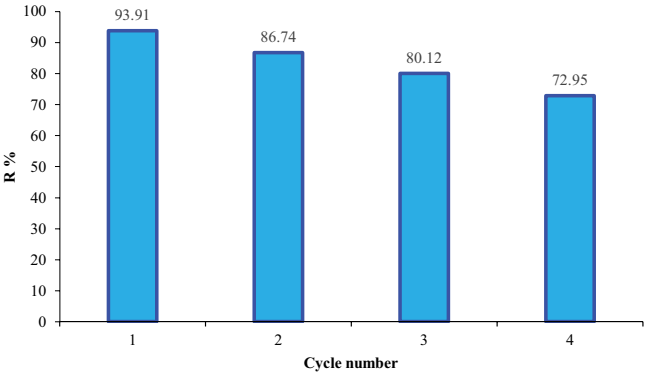

Fig. 16. Reusability study for adsorption methylene blue by ASLP.

[55], as well as aromatic rings responsible for the interaction between the MB dye and the ASLP biosorbent. Fig. 15 presents a proposed interaction mechanism. Four potential adsorption mechanisms were suggested [27,55,56]:

- Hydrogen bonding: The hydroxyl groups (H-donors) in ASLP can form hydrogen bonds with the nitrogen atom of MB (H-acceptors).
- n–π interactions: Oxygen or nitrogen atoms in ASLP can engage in n–π interactions with the aromatic rings of MB.
- Electrostatic attraction: The interaction between the cationic dye MB and the negatively charged groups on the surface of ASLP results in electrostatic attractions.
- π–π interactions: The aromatic structure of ASLP can undergo π–π dispersion interactions with the aromatic ring of MB.

Furthermore, as depicted in Fig. 15, the carboxylic functions become deprotonated, generating negative charges (–COO–) that form bonds with the positively charged MB molecules (N^+).

3.5. Desorption studies

Reusability plays a significant role in minimizing the costs associated with adsorption by allowing for the regeneration of adsorbent materials [57]. The reusability of the adsorbent was evaluated through adsorption–desorption cycles. Desorption of the MB dye was achieved using 0.1 N HCl, and the efficiency was determined using Eq. (4). In the first cycle, a desorption rate of 93.9% was achieved. Even after four cycles, the percentage of desorption did not decrease below 70%. The results of the adsorption–desorption tests are presented in Fig. 16. Similar results were reported for the regeneration of other lignocellulosic compounds utilized in MB adsorption [58]. These results indicate that ASLP can be reused effectively and applied for wastewater treatment purposes.

4. Conclusion

In the present study, a new, cost-effective biosorbent derived from *A. saligna* leaf powder (ASLP) has been investigated to remove MB dye. The adsorption process was found to be influenced by various parameters such as pH, ASLP dose, MB concentration, contact time, and temperature. The presence of hydroxyl, carboxyl, and amine groups on the surface of the adsorbent facilitated the adsorption of MB by providing active sites. Kinetic data analysis revealed that the pseudo-second-order model exhibited the best fit, as indicated by the high regression coefficient values (R^2). The maximum monolayer adsorption capacity was determined to be 71.43 $mg \cdot g^{-1}$. The adsorption isotherm study demonstrated that the Langmuir model provided the best fit for the experimental data. Furthermore, the thermodynamic analysis revealed negative values for $\Delta G°$, $\Delta S°$, and $\Delta H°$, indicating that the adsorption process was spontaneous, feasible, and exothermic. The investigation on reusability confirmed the effectiveness of ASLP in MB dye treatment, as the adsorption capacity only slightly decreased (70%) after the fourth cycle compared to the initial cycle (93.9%). Therefore, ASLP can be successfully reused without significant loss in its adsorption performance. Consequently, it can be concluded that raw *A. saligna* leaf powder serves as an efficient, cost-effective, economically attractive, and readily available biosorbent for the removal of MB from wastewater.

Acknowledgements

The authors thank the Algerian National Administration of Scientific Research (DG-RSDT) for financial support.

Conflicts of interest

The authors declare that they have no conflicts to interest.

References

[1] C. Parvathi, T. Maruthavanan, Adsorptive removal of Megenta MB cold brand reactive dye by modified activated carbons derived from agricultural waste, Indian J. Sci. Technol., 3 (2010) 408–410.
[2] P. Senthil Kumar, S.J. Varjani, S. Suganya, Treatment of dye wastewater using an ultrasonic aided nanoparticle stacked activated carbon: kinetic and isotherm modelling, Bioresour. Technol., 250 (2018) 716–722.
[3] Z. Huang, Y. Li, W. Chen, J. Shi, Y. Zhang, Modified bentonite adsorption of organic pollutants of dye wastewater, Mater. Chem. Phys., 202 (2017) 266–276.

[4] A.H. Jawad, A.M. Kadhum, Y. Ngoh, Applicability of dragon fruit (*Hylocereus polyrhizus*) peels as low-cost biosorbent for adsorption of methylene blue from aqueous solution: kinetics, equilibrium and thermodynamics studies, Desal. Water. Treat., 109 (2018) 231–240.
[5] J. Huang, Y. Cao, Z. Liu, Z. Deng, W. Wang, Application of titanate nanoflowers for dye removal: a comparative study with titanate nanotubes and nanowires, Chem. Eng. J., 191 (2012) 38–44.
[6] D.H.K. Reddy, S.M. Lee, K. Seshaiah, Biosorption of toxic heavy metal ions from water environment using honeycomb biomass—an industrial waste material, Water Air Soil Pollut., 223 (2012) 5967–5982.
[7] M.M. Abd El-Latif, A.M. Ibrahim, M.F. El-Kady, Adsorption equilibrium, kinetics and thermodynamics of methylene blue from aqueous solutions using biopolymer oak sawdust composite, J. Am. Sci., 6 (2010) 267–283.
[8] D. Pathania, S. Sharma, P. Singh, Removal of methylene blue by adsorption onto activated carbon developed from *Ficus carica* bast, Arabian J. Chem., 10 (2017) S1445–S1451.
[9] M. Davodi, H. Alidadi, A. Ramezani, F. Jamali-Behnam, Z. Bonyadi, Study of the removal efficiency of arsenic from aqueous solutions using *Melia azedarach* sawdust modified with FeO: isotherm and kinetic studies, Desal. Water Treat., 137 (2019) 292–299.
[10] S. Nethaji, A. Sivasamy, A.B. Mandal, Adsorption isotherms, kinetics and mechanism for the adsorption of cationic and anionic dyes onto carbonaceous particles prepared from *Juglans regia* shell biomass, Int. J. Environ. Sci. Technol., 10 (2013) 231–242.
[11] I. Anastopoulos, G.Z. Kyzas, Agricultural peels for dye adsorption: a review of recent literature, J. Mol. Liq., 200 (2014) 381–389.
[12] L. Ding, B. Zou, W. Gao, Q. Liu, Z. Wang, Y. Guo, X. Wang, Y. Liu, Adsorption of Rhodamine-B from aqueous solution using treated rice husk-based activated carbon, Colloids Surf., A, 446 (2014) 1–7.
[13] J. Liu, Z. Wang, H. Li, C. Hu, P. Raymer, Q. Huang, Effect of solid-state fermentation of peanut shell on its dye adsorption performance, Bioresour. Technol., 249 (2018) 307–314.
[14] V. Ponnusami, S. Vikram, S.N. Srivastava, Guava (*Psidium guajava*) leaf powder: novel adsorbent for removal of methylene blue from aqueous solutions, J. Hazard. Mater., 152 (2008) 276–286.
[15] A. Nowak-Wegrzyn, A.W. Burks, H.A. Sampson, Food Allergy and Gastrointestinal Syndromes, Middleton's Allergy Essentials, Elsevier, Department of Allergy, Immunology, and Respiratory Medicine Alfred Hospital Monash University, Melbourne, Australia, 2017, pp. 301–343.
[16] A. Kheloufi, Z.F. Boukhatem, L. Mansouri, M. Djelilate, Inventory and geographical distribution of Acacia Mill. (*Fabaceae Mimosaceae*) species in Algeria, Biodivers. J., 9 (2018) 51–60.
[17] J.S. Noh, J.A. Schwarz, Estimation of the point of zero charge of simple oxides by mass titration, J. Colloid Interface Sci., 130 (1989) 157–164.
[18] S.M. Anisuzzaman, C.G. Joseph, Y.H. Taufiq-Yap, D. Krishnaiah, V.V. Tay, Modification of commercial activated carbon for the removal of 2,4-dichlorophenol from simulated wastewater, J. King Saud Univ. Sci., 27 (2015) 318–330.
[19] G.A. Parks, Chapter 4. Surface Energy and Adsorption at Mineral/Water Interfaces: An Introduction, M.F. Hochella, A.F. White, Eds., Mineral-Water Interface Geochemistry, De Gruyter, Berlin, Boston, 2018, pp. 133–176.
[20] D.S. Malik, C.K. Jain, A.K. Yadav, G.K. Vishwavidyalaya, Preparation and characterization of plant based low-cost adsorbents, J. Global Biosci., 4 (2015) 1824–1829.
[21] D. Kibami, P. Chubaakum, K.S. Rao, S. Dipak, Preparation and characterization of activated carbon from *Fagopyrum esculentum* Moench by HNO_3 and H_3PO_4 chemical activation, Der Chem. Sin., 5 (2014) 46–55.
[22] E. Papirer, E. Guyon, N. Perol, Contribution to the study of the surface groups on carbons—II: spectroscopic methods, Carbon, 16 (1978) 133–140.
[23] M.T. Yagub, T.K. Sen, H.M. Ang, Equilibrium, kinetics, and thermodynamics of methylene blue adsorption by pine tree leaves, Water Air Soil Pollut., 223 (2012) 5267–5282.
[24] N.P. Adetya, U.F. Arifin, E. Anggriyani, The removal of chromium(VI) from tannery waste using *Spirulina* sp. immobilized silica gel, Turk. J. Chem., 45 (2021) 1854–1864.
[25] H. Lin, K. Chen, L. Du, P. Gao, J. Zheng, Y. Liu, L. Ma, Efficient and selective adsorption of methylene blue and methyl violet dyes by yellow passion fruit peel, Environ. Technol., 43 (2022) 3519–3530.
[26] W. Hassan, U. Farooq, M. Ahmad, M. Athar, M.A. Khan, Potential biosorbent, *Haloxylon recurvum* plant stems, for the removal of methylene blue dye, Arabian J. Chem., 10 (2017) S1512–S1522.
[27] O. Sulaiman, M.H.M. Amini, M. Rafatullah, R. Hashim, A. Ahmad, Adsorption equilibrium and thermodynamic studies of copper(II) ions from aqueous solutions by oil palm leaves, Int. J. Chem. React. Eng., (2010) 8, doi: 10.2202/1542-6580.2350.
[28] X. Han, X. Niu, X. Ma, Adsorption characteristics of methylene blue on poplar leaf in batch mode: equilibrium, kinetics and thermodynamics, Korean J. Chem. Eng., 29 (2012) 494–502.
[29] M.C. Terkhi, F. Taleb, P. Gossart, A. Semmoud, A. Addou, Fourier transform infrared study of mercury interaction with carboxyl groups in humic acids, J. Photochem. Photobiol., A, 198 (2008) 205–214.
[30] M. Mathivanan, S. Syed Abdul Rahman, R. Vedachalam, S. Karuppiah, *Ipomoea carnea*: a novel biosorbent for the removal of methylene blue (MB) from aqueous dye solution: kinetic, equilibrium and statistical approach, Int. J. Phytorem., 23 (2021) 982–1000.
[31] N.M. Nurazzi, M.R.M. Asyraf, M. Rayung, M.N.F. Norrrahim, S.S. Shazleen, M.S.A. Rani, A.R. Shafi, H.A. Aisyah, M.H.M. Radzi, F.A. Sabaruddin, R.A. Ilyas, E.S. Zainudin, K. Abdan, Thermogravimetric analysis properties of cellulosic natural fiber polymer composites: a review on influence of chemical treatments, Polymers, 13 (2021) 2710, doi: 10.3390/polym13162710.
[32] N.B.R. Legrand, M. Lucien, O. Pierre, B.E. Fabien, N.P. Marcel, A.A. Jean, Physico-chemical and thermal characterization of a lignocellulosic fiber, extracted from the bast of *Cola lepidota* stem, J. Miner. Mater. Charact. Eng., 8 (2020) 377–392.
[33] H. Yang, R. Yan, H. Chen, H. Dong, H.D. Lee, C. Zheng, Characteristics of hemicellulose, cellulose and lignin pyrolysis, Fuel, 86 (2007) 1781–1788.
[34] Z. Aksu, Application of biosorption for the removal of organic pollutants: a review, Process Biochem., 40 (2005) 997–1026.
[35] A. Ouldmoumna, L. Reinert, N. Benderdouche, B. Bestani, L. Duclaux, Characterization and application of three novel biosorbents "*Eucalyptus globulus*, *Cynara cardunculus*, and *Prunus cerasefera*" to dye removal, Desal. Water Treat., 51 (2013) 3527–3538.
[36] W. Zou, H. Bai, S. Gao, K. Li, Characterization of modified sawdust, kinetic and equilibrium study about methylene blue adsorption in batch mode, Korean J. Chem. Eng., 30 (2013) 111–122.
[37] E.F.D. Januário, T.B. Vidovix, L.A.D. Araújo, L. Bergamasco Beltran, R. Bergamasco, A.M.S. Vieira, Investigation of *Citrus reticulata* peels as an efficient and low-cost adsorbent for the removal of safranin orange dye, Environ. Technol., 43 (2022) 4315–4329.
[38] H.M.F. Freundlich, Over the adsorption in solution, J. Phys. Chem., 57 (1906) 1100–1107.
[39] S.K. Lagergren, About the theory of so-called adsorption of soluble substances, Sven. Vetenskapsakad, Handingarl, 24 (1898) 1–39.
[40] Y.S. Ho, G. McKay, Kinetic models for the sorption of dye from aqueous solution by wood, Process Saf. Environ. Prot., 76 (1998) 183–191.
[41] W.J. Weber, J.C. Morris, Kinetic of adsorption on carbon from solution, J. Sanit. Eng. Div., 89 (1963) 31–59.

[42] B. Bestani, N. Benderdouche, B. Benstaali, M. Belhakem, A. Addou, Methylene blue and iodine adsorption onto an activated desert plant, Bioresour. Technol., 99 (2008) 8441–8444.
[43] T.K. Sen, S. Afroze, H.M. Ang, Equilibrium, kinetics and mechanism of removal of methylene blue from aqueous solution by adsorption onto pinecone biomass of *Pinus radiate*, Water Air Soil Pollut., 218 (2011) 499–515.
[44] I. Langmuir, The constitution and fundamental properties of solids and liquids. Part I. Solids, J. Am. Chem. Soc., 38 (1916) 2221–2295.
[45] P.O. Boamah, Q. Zhang, M. Hua, Y. Huang, Y. Liu, W. Wang, Y. Liu, Lead removal onto cross-linked low molecular weight chitosan pyruvic acid derivatives, Carbohydr. Polym., 110 (2014) 518–527.
[46] R. Han, W. Zou, W. Yu, S. Cheng, Y. Wang, J. Shi, Biosorption of methylene blue from aqueous solution by fallen phoenix tree's leaves, J. Hazard. Mater., 141 (2007) 156–162.
[47] K.G. Bhattacharyya, A. Sharma, Kinetics and thermodynamics of methylene blue adsorption on neem (*Azadirachta indica*) leaf powder, Dyes Pigm., 65 (2005) 51–59.
[48] S.A. Ansari, F. Khan, A. Ahmad, Cauliflower leave, an agricultural waste biomass adsorbent, and its application for the removal of MB dye from aqueous solution: equilibrium, kinetics, and thermodynamic studies, Int. J. Anal. Chem., 2016 (2016) 1–10.
[49] Z. Bingul, E. Adar, Usability of spent *Salvia officinalis* as a low-cost adsorbent in the removal of toxic dyes: waste assessment and circular economy, Int. J. Environ. Anal. Chem., (2021) 1–16, doi: 10.1080/03067319.2021.1949588.
[50] B.T. Gemici, H.U. Ozel, H.B. Ozel, Removal of methylene blue onto forest wastes: adsorption isotherms, kinetics and thermodynamic analysis, Environ. Technol. Innovation, 22 (2021) 101501, doi: 10.1016/j.eti.2021.101501.
[51] C. Ammar, Y. El-Ghoul, M. Jabli, Characterization and valuable use of *Calotropis gigantea* seedpods as a biosorbent of methylene blue, Int. J. Phytorem., 23 (2021) 1085–1094.
[52] R. Fiaz, M. Hafeez, R. Mahmood, *Ficcus palmata* leaves as a low-cost biosorbent for methylene blue: thermodynamic and kinetic studies, Water Environ. Res., 91 (2019) 689–699.
[53] M. Kerrou, N. Bouslamti, A. Raada, A. Elanssari, D. Mrani, M.S. Slimani, The use of sugarcane bagasse to remove the organic dyes from wastewater, Int. J. Anal. Chem., 2021 (2021) 1–11.
[54] Z. Belala, M. Jeguirim, M. Belhachemi, F. Addoun, G. Trouvé, Biosorption of basic dye from aqueous solutions by date stones and palm-trees waste: kinetic, equilibrium and thermodynamic studies, Desalination, 271 (2011) 80–87.
[55] R.N. Oliveira, M.C. Mancini, F.C.S. Oliveira, T.M. Passos, B. Quility, R.M.S. Thire, G.B. Mcguiness, FTIR analysis and quantification of phenols and flavonoids of five commercially available plants extracts used in wound healing, Rev. Mater., 21 (2016) 767–779.
[56] H.N. Tran, S.J. You, T.V. Nguyen, H.P. Chao, Insight into the adsorption mechanism of cationic dye onto biosorbents derived from agricultural wastes, Chem. Eng. Commun., 204 (2017) 1020–1036.
[57] H.E. Ezerie, R.M.K. Shamsul, M. Amirhossein, H. Mohamed, Characterization and optimization of effluent dye removal using a new low-cost adsorbent: equilibrium, kinetics and thermodynamic study, Process Saf. Environ. Prot., 98 (2015) 16–32.
[58] J. Bortoluz, F. Ferrarini, L.R. Bonetto, J. da Silva Crespo, M. Giovanela, Use of low-cost natural waste from the furniture industry for the removal of methylene blue by adsorption: isotherms, kinetics and thermodynamics, Cellulose, 27 (2020) 6445–6466.